J. Fluid Mech. (1994), vol. 265, pp. 245–263

Stability of inviscid conducting liquid columns subjected to a.c. axial magnetic fields

By ANTONIO CASTELLANOS[1] AND HELIODORO GONZÁLEZ[1,2]

[1] Departamento Electrónica y Electromagnetismo, Universidad de Sevilla, Spain

[2] Departamento Física Aplicada, Universidad de Sevilla, Spain

(Received 8 February 1993 and in revised form 22 October 1993)

The natural frequencies and stability criterion for cylindrical inviscid conducting liquid bridges and jets subjected to axial alternating magnetic fields in the absence of gravity are obtained. For typical conducting materials a frequency greater than 100 Hz is enough for a quasi-steady approximation to be valid. On the other hand, for frequencies greater than 10^5 Hz an inviscid model may not be justified owing to competition between viscous and magnetic forces in the vicinity of the free surface. The stability is governed by two independent parameters. One is the magnetic Bond number, which measures the relative influence of magnetic and capillary forces, and the other is the relative penetration length, which is given by the ratio of the penetration length of the magnetic field to the radius. The magnetic Bond number is proportional to the squared amplitude of the magnetic field and inversely proportional to the surface tension. The relative penetration length is inversely proportional to square root of the product of the frequency of the applied field and the electrical conductivity of the liquid. It is shown in this work that stability is enhanced by either increasing the magnetic Bond number or decreasing the relative penetration length.

1. Introduction

The motivation for this work is the enhancement of the stabilization of the free interface of the molten zone in the crucible-free float zone technique. In this technique a liquid bridge is formed between the solidification and melting front interfaces of an ingot rod, locally heated. In the absence of gravity, capillary forces are able to hold a cylindrical bridge if its length L does not exceed its perimeter $2\pi R$, R being the radius of the cylinder (Rayleigh's criterion). For insulating liquids it is possible to increase substantially the maximum length attainable using dielectric forces (González *et al.* 1989). Application of intense electric fields is not possible for semiconductor materials (Si, GaAs), owing to their high conductivity in the molten phase. For these cases, which are of the greatest technological interest, magnetic forces could be of help to stabilize the melted zone. In fact, earlier researchers and users of the float zone technique for growing high-purity silicon crystals were well aware of the stabilizing effect of magnetic forces (Keller & Mühlbauer 1981). These forces appear naturally in the system when radio-frequency magnetic fields are used to heat by induction and melt the polycrystalline feed rod. According to the same authors a crude estimation of the supporting electrodynamic pressure for a molten silicon column with $R = 2.5$ cm, to which an input electrical power of 4 kW with a frequency of 4 MHz is applied, gives $p = 2.13$ mbar, to be compared to the pressure $p = 0.32$ mbar due to surface tension.

The electrodynamic pressure is probably overestimated, but based on this argument and empirical observations, Keller & Mühlbauer recommend induction heating as the most beneficial heating method for semiconducting materials. In real situations the melted rod is subjected to instabilities due to variations in surface tension induced by thermal gradients, residual gravity, rotation, axial acceleration, etc. (see Hurle, Müller & Nitsche 1987 and references therein). Here we shall consider an idealized situation in which these complications are disregarded in order to understand the physics due to the magnetic field. The physical configuration that we present in the next section envisages a laboratory experiment not directly related to the floating zone technique. Nevertheless, in our opinion, the results may be also of interest for this technique.

Notwithstanding the practical importance of magnetic forces, very few detailed theoretical studies have been devoted to this subject. It is interesting to note that a long time ago, Chandrasekhar, in a classical study, demonstrated that for a jet of a perfectly conducting liquid both the critical wavenumber and the initial growth rate of the most unstable disturbance decrease as the strength of a steady magnetic field increases (Chandrasekhar 1961). During the completion of this work we have become aware of another paper (Nicolás 1992) that extends these results to the liquid bridge configuration. Nevertheless, as pointed out by Chandrasekhar, the stabilizing effect of axial steady magnetic fields for liquid metal (or molten semiconductor) bridges is negligibly small owing to their finite conductivity.

Recently, an interesting work has been published, where the authors (Riahi & Walker 1989) discuss the effect of magnetic forces upon the shape and stability of a liquid zone, considering a magnetic field generated by a single coil. In their paper the induction coil is idealized as a line current so close to the float zone that locally the surface may be considered as planar and the method of images is applied to determine the value of the magnetic field outside the rod. The frequency is high enough to treat the outer problem as a magnetohydrostatic one, with zero magnetic field inside the melted zone. It is readily apparent from the analysis that the magnetic field (tangential to the interface) plays a stabilizing role, but the pinch effect may destabilize the float zone, past a critical value of the magnetic field, by spilling the melt at the point where the melted zone intersects the crystal phase. Garnier & Moreau (1983), motivated by shape control, stability and purification problems in the continuous casting of liquid metals, have also demonstrated the positive influence of tangential alternating fields on the stability of planar interfaces. They have shown by means of an inviscid model that for a given magnetic field intensity, the stability increases as the frequency is increased.

In this paper we extend the work of Garnier & Moreau to cylindrical interfaces, particularized to vacuum as the outer media. We also discuss the validity of an inviscid approach. We consider the stability of liquid columns, either of finite length (liquid bridges) or infinite length (jets). Contrary to the case of a planar interface, it is now the capillary instability mechanism that is responsible for the breaking of the column in the absence of magnetic field. Moreover, in the liquid bridge configuration there are two new distances, the radius of the liquid bridge R and the distance between the supporting solids L, in addition to the penetration length of the field $\delta \equiv (\omega\mu_0 \sigma_e)^{-\frac{1}{2}}$ (ω is the angular frequency of the applied magnetic field). Thus, two new parameters $d = \delta/R$, the relative penetration length, and $\Lambda = L/2R$, the slenderness, enter into the formulation of the problem. The boundary conditions at the solid–liquid interfaces make the analysis more involved as the whole set of natural oscillation modes of the jet are coupled. With respect to the anchoring conditions, a free contact angle is assumed to allow an exact analytical treatment of the problem. The dispersion relation of the jet is obtained separately because in the limit of L going to infinity the modes pertaining to the liquid bridge configuration remain coupled. The limit of the radius going to infinity is obtained and a comparison with the results of Garnier & Moreau is made.

For the problem that we shall deal with, some simplifications can be made from dimensional arguments based upon the values of the physical constants of typical molten semiconductors, or liquid metals. The equation governing the magnetic field is, from Maxwell's equations,

$$\nabla \times \nabla \times \boldsymbol{H} = -\sigma_e \mu_0 \frac{\partial \boldsymbol{H}}{\partial t} + \sigma_e \mu_0 \nabla \times (\boldsymbol{v} \times \boldsymbol{H}) - \epsilon_0 \mu_0 \frac{\partial^2 \boldsymbol{H}}{\partial t^2}, \tag{1}$$

where we assume that the conducting liquid is essentially a non-polarizable and non-magnetizable media, and that the constitutive law for the current density is $\boldsymbol{j} = \sigma_e(\boldsymbol{E} + \mu_0 \boldsymbol{v} \times \boldsymbol{H})$, with ϵ_0 and μ_0 the vacuum permittivity and permeability respectively, σ_e the electrical conductivity and $\boldsymbol{E}$ the electric field. As is well known, the radiative term, $\epsilon_0 \mu_0 \partial^2 \boldsymbol{H}/\partial t^2$, is negligibly small in the radio-frequency range. The ratio of the convective term, $\sigma_e \mu_0 \nabla \times (\boldsymbol{v} \times \boldsymbol{H})$, to the diffusive term, $\sigma_e \mu_0 \partial \boldsymbol{H}/\partial t$, is of the order of $R/\delta f t_c$, where $f = \omega/2\pi$, and $t_c = (\rho R^3/\sigma)^{\frac{1}{2}}$, ρ being the mass density and σ the surface tension. According to this simple dimensional argument, for $R = 2$ cm and $f > 100$ Hz, (1) may be reduced to

$$\nabla \times \nabla \times \boldsymbol{H} = -\sigma_e \mu_0 \frac{\partial \boldsymbol{H}}{\partial t}, \tag{2}$$

where it has been assumed that the liquid velocity is not larger than R/t_c.

In what follows the diffusive term will be kept as we are interested in studying the effect of alternating magnetic fields on the stability of our system.

On the other hand, for a liquid bridge of radius R, the Reynolds numbers $Re \equiv \delta^2/\nu t_c$ (ν is the kinematic viscosity) is given by the ratio of the inertial term to the viscous term, or equivalently as the ratio of the vorticity diffusion time to the mechanical one, where this latter is based on the capillary forces. Spatial variations of the velocity are estimated using the penetration length because the magnetic forces are concentrated in a narrow region adjacent to the interface and cause strong variations in pressure and radial velocity (see figure 4 below). Molten silicon at a temperature of 1690 K has a density $\rho = 2.530 \times 10^3$ kg m^{-3}, surface tension $\sigma = 0.8$ N m^{-1}, kinematic viscosity $\nu = 0.35 \times 10^{-6}$ m s^{-2} (Martínez & Cröll 1992) and electrical conductivity $\sigma_e = 1.11 \times 10^6$ S m^{-1} (Keller & Mühlbauer 1981). For a liquid bridge of radius $R = 2 \times 10^{-2}$ m subjected to magnetic fields of frequency $f = 10^5$ Hz, we find $t_c = 0.16$ s, $\delta = 10^{-3}$ m and consequently $Re = 20$, so that an inviscid approximation could be justified. However, greater frequencies result in lower Reynolds number so that there exists competition between magnetic and viscous forces in the skin-depth layer.

This paper is organized as follows. Section 2 is devoted to the physical system under investigation, the governing equations and the basic hydrostatic solution. In §3 a linear model is developed to give the dynamical response of the bridge to small perturbations, including the stability criterion as a function of the relevant parameters. The limit of imposed fields of infinite frequency is considered at the end of the section and serves as a test of the previous calculations. The case of the jet is treated separately in §4 owing to its theoretical importance. In §5 we discuss the dependence on parameters for the natural frequencies and stability of the jet and liquid bridge. Finally in §6 the main conclusions are drawn.

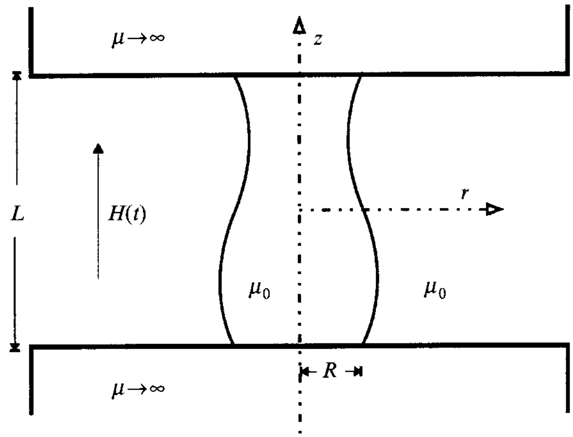

FIGURE 1. Schematic of the physical system, indicating relevant physical parameters.

2. Formulation of the problem

Let us consider a conducting liquid column of radius R in zero-gravity conditions anchored between two parallel planes a distance L apart and surrounded by a gaseous ambient. Such a configuration is known in the literature as a liquid bridge. We assume that the contact line is fixed with free contact angle. In a possible laboratory experiment free contact angles might be achieved by using sharp-edged supporting disks to anchor the bridge. The liquid volume is fixed at $V = \pi R^2 L$. We model the liquid as having electrical conductivity σ_e, density ρ, the vacuum permeability μ_0, and surface tension σ, and finally we assume that it is incompressible and inviscid. The surrounding gas also has the vacuum permeability and a negligible density compared with that of the liquid.

The liquid bridge is located between the parallel poles of a large section electromagnet, so that a uniform alternating magnetic field of frequency ω is imposed over a wide region including the bridge. Therefore, for regions inside the electromagnet gap but far from the liquid column the magnetic field is written $\boldsymbol{H}_\infty(t) = H_0 \cos(\omega t)\, \boldsymbol{e}_z$, where we use cylindrical coordinates (r, z) defined in figure 1. We restrict ourselves to axisymmetric geometries of the liquid surface, which we represent by

$$F(r, z, t) \equiv r - f(z, t) = 0. \tag{3}$$

Outside the liquid zone there is no current and the magnetic field $\boldsymbol{H}^o$ is derived from a harmonic potential:

$$\boldsymbol{H}^o = \nabla\phi, \quad \nabla^2\phi = 0. \tag{4}$$

Inside the conducting liquid the equations governing the magnetic field $\boldsymbol{H}^i$, according to the discussion in the introduction, are

$$\nabla \cdot \boldsymbol{H}^i = 0, \tag{5}$$

$$\nabla \times \nabla \times \boldsymbol{H}^i + \sigma_e \mu_0 \frac{\partial \boldsymbol{H}^i}{\partial t} = 0. \tag{6}$$

The dynamics of the outer medium is fully described by a constant pressure p^o, because of the assumption of negligible gas density. In the liquid region we have pressure and velocity fields, $p(r, z, t)$ and $\boldsymbol{v}(r, z, t)$ respectively, governed by the continuity equation for the incompressible case and the Euler equation including a magnetic force term:

$$\nabla\cdot\boldsymbol{v} = 0, \tag{7}$$

$$\rho\frac{\partial \boldsymbol{v}}{\partial t}+\rho\boldsymbol{v}\cdot\nabla\boldsymbol{v} = -\nabla p+\mu_0(\nabla\times\boldsymbol{H}^i)\times\boldsymbol{H}^i. \tag{8}$$

Using the identity $(\nabla\times\boldsymbol{H}^i)\times\boldsymbol{H}^i = (\boldsymbol{H}^i\cdot\nabla)\,\boldsymbol{H}^i-\frac{1}{2}\nabla H^{i2}$ and (5) we can rewrite (8) in the form

$$\rho\frac{\partial \boldsymbol{v}}{\partial t}+\rho\boldsymbol{v}\cdot\nabla\boldsymbol{v} = -\nabla\Pi+\mu_0(\boldsymbol{H}^i\cdot\nabla)\,\boldsymbol{H}^i, \tag{9}$$

with Π given by

$$\Pi\equiv p+\tfrac{1}{2}\mu_0(\nabla H^i)^2. \tag{10}$$

Taking the divergence of (9) and using (7) we find

$$\rho\nabla\cdot(\boldsymbol{v}\cdot\nabla\boldsymbol{v}) = -\nabla^2\Pi+\mu_0\,\nabla\cdot[(\boldsymbol{H}^i\cdot\nabla)\,\boldsymbol{H}^i]. \tag{11}$$

To define completely the mathematical problem we must impose the following boundary conditions.

(i) At the planes $z = \pm\frac{1}{2}L$

$$v_z = 0,\quad H_r^i = H_r^o = 0, \tag{12}$$

i.e. the fluid does not penetrate into the magnet and there the tangential component of the magnetic field is zero.

(ii) At the symmetry axis, $\boldsymbol{H}^i$, p and $\boldsymbol{v}$ must be non-singular.

(iii) At the free surface $F(r,z,t) = 0$, the magnetic field is continuous,

$$\boldsymbol{H}^i(f(z,t),z,t) = \boldsymbol{H}^o(f(z,t),z,t), \tag{13}$$

the liquid surface is attached to the fluid motion (kinematic condition), i.e.

$$\frac{\partial F}{\partial t}+\boldsymbol{v}\cdot\nabla F = 0, \tag{14}$$

and the normal stress jump is equal to the capillary jump,

$$p^i(f(z,t),z,t)-p^o = \sigma(1/R_1+1/R_2), \tag{15}$$

where R_1 and R_2 are the principal radii of curvature at a given surface point, which we can calculate by defining a unit normal vector to the free surface as the function

$$\boldsymbol{n} = \frac{\nabla F}{|\nabla F|} \tag{16}$$

evaluated at $F = 0$. Then, the mean curvature of the surface is $(1/R_1+1/R_2) = \nabla\cdot\boldsymbol{n}$ also evaluated at $F = 0$.

In the last equation the jump in the normal magnetic stress does not appear because the magnetic properties of both media are identical and the field is continuous. More precisely, the magnetic stress applied on a surface point is

$$\mu_0(H_n^o\,\boldsymbol{H}^o-\tfrac{1}{2}H^{o2}\boldsymbol{n})-\mu_0(H_n^i\,\boldsymbol{H}^i-\tfrac{1}{2}H^{i2}\boldsymbol{n}), \tag{17}$$

where $H_n^o = \boldsymbol{H}^o\cdot\boldsymbol{n}$. The magnetic stress is zero because of (13). On the other hand, this result makes the problem compatible with the inviscid approximation. Otherwise, the effects of viscosity would be needed to compensate the tangential stresses.

It is convenient to express (15) in terms of the modified pressure Π. Using the continuity of the magnetic field across the free surface we have

$$\Pi - p^o - \mu_0 H^{o2} = \sigma \nabla \cdot \boldsymbol{n}. \tag{18}$$

Finally, preservation of the cylindrical volume leads to the following constraint for the shape of the bridge:

$$\int_{-L/2}^{L/2} \mathrm{d}z f(z)^2 = LR^2. \tag{19}$$

The magneto-mechanical problem formulated above admits a hydrostatic solution ($\boldsymbol{v}_S = 0$) represented by a cylindrical shape of radius R and a magnetic field which is uniform in the outer region and diffuses to some extent into the conducting liquid:

$$f_S = R; \quad \boldsymbol{H}_S^o = H_0 \cos \omega t \boldsymbol{e}_z, \tag{20}$$

$$\boldsymbol{H}_S^i = H_S \boldsymbol{e}_z = H_0 \operatorname{Re}\left[\frac{I_0(\mathrm{i}^{\frac{1}{2}} r/\delta)}{I_0(\mathrm{i}^{\frac{1}{2}}/\delta)} \mathrm{e}^{\mathrm{i}\omega t}\right] \boldsymbol{e}_z \tag{21}$$

$$\Pi_S = p^o + \frac{\sigma}{R} + \mu_0 H_0^2 \cos^2 \omega t, \tag{22}$$

where Re stands for the real part of the argument, I_0 is the modified Bessel function of the first kind and δ, already introduced, is the penetration length in the conducting liquid for the imposed a.c. magnetic field. The case of a jet corresponds to a liquid bridge of infinite length for which the boundary conditions (12) no longer apply.

3. Small-oscillation analysis for the liquid bridge

We are interested in the stability with respect to small disturbances of the static solution. When the free surface is deformed, no other hydrostatic solution, i.e. with zero velocity field, is possible. This is apparent by taking the curl of the magnetic force in (8), which is in general non-zero for a non-homogeneous magnetic field and consequently the velocity has vectorial sources. Static analysis is possible only when, for any equilibrium shape we have $\boldsymbol{v} = 0$, which is not the case except for the limit of infinite imposed field frequency ω, which will be discussed at the end of this section.

Let us perturb the free surface in the form

$$f(z,t) = R + \operatorname{Re}[\epsilon f_0(z) \mathrm{e}^{\mathrm{i}st}], \tag{23}$$

with $\epsilon \ll R$, which represents a generic normal mode with natural frequency s. Any arbitrary small disturbance of the liquid shape may be written as a linear combination of these modes. We assume that ϵ is a good parameter to expand any other magnitude describing the system. However, we cannot adopt the same time dependence for all quantities because the imposed magnetic field has his own timescale.

3.1. *Time dependences*

As in Garnier & Moreau (1983), equation (13) gives the condition that relates the surface shape and the perturbed magnetic fields. Putting

$$\boldsymbol{H}^i = \boldsymbol{H}_S^i(r,t) + \epsilon \boldsymbol{h}_0(r,z,t), \tag{24}$$

$$\boldsymbol{H}^o = \boldsymbol{H}_S^o(r,t) + \epsilon \nabla \phi_0(r,z,t) \tag{25}$$

and substituting in the tangential component of (13) we obtain the following linearized condition:

$$\mathrm{Re}\,[f_0\,\mathrm{e}^{\mathrm{i}st}]\left[\frac{\mathrm{i}^{\frac{1}{2}}/\delta I_1(\mathrm{i}^{\frac{1}{2}}R/\delta)}{I_0(\mathrm{i}^{\frac{1}{2}}/\delta)}\mathrm{e}^{\mathrm{i}\omega t}+\frac{(-\mathrm{i})^{\frac{1}{2}}/\delta I_1((-\mathrm{i})^{\frac{1}{2}}R/\delta)}{I_0((-\mathrm{i})^{\frac{1}{2}}/\delta)}\mathrm{e}^{-\mathrm{i}\omega t}\right]+h_{0z}=\frac{\partial\phi_0}{\partial z}(R,z). \quad (26)$$

The first term in the left-hand side of this equation introduces the product of both existing time dependences. The natural choices for the perturbed magnetic fields are

$$\boldsymbol{h}_0(r,z,t)=\mathrm{Re}\,[\boldsymbol{h}_+(r,z)\,\mathrm{e}^{\mathrm{i}(s+\omega)t}+\boldsymbol{h}_-(r,z)\,\mathrm{e}^{\mathrm{i}(s-\omega)t}], \quad (27)$$

$$\phi_0(r,z,t)=\mathrm{Re}\,[\phi_+(r,z)\,\mathrm{e}^{\mathrm{i}(s+\omega)t}+\phi_-(r,z)\,\mathrm{e}^{\mathrm{i}(s-\omega)t}]. \quad (28)$$

Now we have two independent problems for the complex spatial functions $\boldsymbol{h}_+(r,z)$, $\phi_+(r,z)$ and $\boldsymbol{h}_-(r,z)$, $\phi_-(r,z)$, namely

$$\nabla^2\phi_\pm=0 \quad (29)$$

for the outer region and

$$(\nabla^2\mp\mathrm{i}/\delta_\pm^2)\,\boldsymbol{h}_\pm=0, \quad (30)$$

$$\boldsymbol{\nabla}\cdot\boldsymbol{h}_\pm=0 \quad (31)$$

for the inner region, where $\delta_\pm\equiv[\mu_0\,\sigma_e(\omega\pm s)]^{-\frac{1}{2}}$. The boundary conditions are

$$h_{\pm,r}(R,z)=\frac{\partial\phi_\pm}{\partial r}(R,z), \quad (32)$$

$$h_{\pm,z}-\frac{\partial\phi_\pm}{\partial z}=\tfrac{1}{2}f_0(z)\frac{(\pm\mathrm{i})^{\frac{1}{2}}R}{\delta}\frac{I_1((\pm\mathrm{i})^{\frac{1}{2}}R/\delta)}{I_0((\pm\mathrm{i})^{\frac{1}{2}}R/\delta)}. \quad (33)$$

Now we focus our attention on the equation for the pressure. The right-hand side has the following first-order term in ϵ:

$$\begin{aligned}\mu_0\,\boldsymbol{\nabla}\cdot[(\boldsymbol{H}_S\cdot\boldsymbol{\nabla})\,\boldsymbol{h}+(\boldsymbol{h}\cdot\boldsymbol{\nabla})\,\boldsymbol{H}_S]&=2\mu_0\frac{\partial H_S}{\partial r}\frac{\partial h_r}{\partial z}\\&=\mu_0\,\mathrm{Re}\left\{\left[\frac{\mathrm{i}^{\frac{1}{2}}r}{\delta}\frac{I_1(\mathrm{i}^{\frac{1}{2}}r/\delta)}{I_0(\mathrm{i}^{\frac{1}{2}}r/\delta)}\mathrm{e}^{\mathrm{i}\omega t}+\frac{(-\mathrm{i})^{\frac{1}{2}}r}{\delta}\frac{I_1((-\mathrm{i})^{\frac{1}{2}}r/\delta)}{I_0((-\mathrm{i})^{\frac{1}{2}}r/\delta)}\mathrm{e}^{-\mathrm{i}\omega t}\right]\right.\\&\qquad\left.\times\left[\frac{\partial h_{+,r}}{\partial z}\mathrm{e}^{\mathrm{i}(s+\omega)t}+\frac{\partial h_{-,r}}{\partial z}\mathrm{e}^{\mathrm{i}(s-\omega)t}\right]\right\}. \quad (34)\end{aligned}$$

As the order of magnitude of s is given by the inverse of the capillary time $t_c=(\rho R^3/\sigma)^{\frac{1}{2}}$, and we have $|s|\ll\omega$, we may calculate the average of (34) over a period of the fast scale $T=2\pi/\omega$ at an arbitrary time t_0:

$$\begin{aligned}\left\langle 2\mu_0\frac{\partial H_S}{\partial r}\frac{\partial h_r}{\partial z}\right\rangle&\equiv\frac{1}{T}\int_{t_0}^{t_0+T}\mathrm{d}t\,2\mu_0\frac{\partial H_S}{\partial r}\frac{\partial h_r}{\partial z}\\&=\mu_0\left[\frac{\mathrm{i}^{\frac{1}{2}}r}{\delta}\frac{I_1(\mathrm{i}^{\frac{1}{2}}r/\delta)}{I_0(\mathrm{i}^{\frac{1}{2}}r/\delta)}\frac{\partial h_{-,r}}{\partial z}+\frac{(-\mathrm{i})^{\frac{1}{2}}r}{\delta}\frac{I_1((-\mathrm{i})^{\frac{1}{2}}r/\delta)}{I_0((-\mathrm{i})^{\frac{1}{2}}r/\delta)}\frac{\partial h_{+,r}}{\partial z}\right]\mathrm{e}^{\mathrm{i}st_0}+O(|s|/\omega). \quad (35)\end{aligned}$$

This resulting time dependence justifies the adoption of the slow timescale for the fluid mechanical magnitudes:

$$\Pi=\Pi_S+\epsilon\Pi_0(r,z)\,\mathrm{e}^{\mathrm{i}st},\quad \boldsymbol{v}=\epsilon\boldsymbol{v}_0(r,z)\,\mathrm{e}^{\mathrm{i}st}, \quad (36)$$

bearing in mind that we neglect a highly pulsating term in the magnetic force (frequency 2ω). This is the main assumption of the quasi-steady approximation.

3.2. *Resolution in volume*

Let us make lengths non-dimensional with R and magnetic fields with H_0. Equations (29)–(31) have the formal solutions in terms of infinite sine and cosine Fourier–Bessel series:

$$\phi_{\pm}(r,z) = \sum_{n=1}^{\infty} \phi_n^{(\pm)} \frac{K_0(x_n r)}{K_0(x_n)} \sin[x_n(z+\Lambda)], \tag{37}$$

$$h_{\pm,z}(r,z) = \sum_{n=0}^{\infty} h_n^{(\pm)} \frac{I_0(k_n^{\pm} r)}{I_0(k_n^{\pm})} \cos[x_n(z+\Lambda)], \tag{38}$$

$$h_{\pm,r}(r,z) = \sum_{n=1}^{\infty} \frac{x_n h_n^{(\pm)}}{k_n^{\pm}} \frac{I_1(k_n^{\pm} r)}{I_0(k_n^{\pm})} \sin[x_n(z+\Lambda)], \tag{39}$$

where $\Lambda \equiv L/2R$ represents the slenderness of the liquid bridge, $x_n \equiv n\pi/2\Lambda$, $k_n^{\pm} \equiv (x_n^2 + iR^2/\delta_{\pm}^2)^{\frac{1}{2}}$ and $\phi_n^{(\pm)}$ and $h_n^{(\pm)}$ are coefficients to be determined from the conditions at the free surface. Implicit use of some boundary conditions has been made to construct these solutions. In particular we have selected the dependence on the axial coordinate to make null the tangential component of the magnetic fields at the electromagnet poles, i.e. $z = \pm\Lambda$, and we have also used conditions of regularity at the symmetry axis and decaying behaviour for increasing r to select the radial dependence in both regions. We will from now on suppress any distinction between both definitions of the penetration depths $\delta_{\pm}$ because $|\omega \pm s| \approx |\omega|$ in the quasi-steady approximation. Thus, only the penetration depth δ is considered everywhere and, on the other hand, k_n^- becomes the complex conjugate of k_n^+.

According to the scaling of lengths with the anchoring radius R, we observe the appearance in the definition of $k_n^{\pm}$ of the non-dimensional parameter δ/R, the 'relative penetration depth'.

We are now in position to solve for the perturbed pressure, which will be made non-dimensional by scaling with the capillary pressure jump σ/R. Equation (11) yields to first order

$$e^{ist} \nabla^2 \Pi_0 = \left\langle 2\mu_0 \frac{\partial H_S}{\partial r} \frac{\partial h_r}{\partial z} \right\rangle. \tag{40}$$

According to (35) and (39) we have an inhomogeneity expressed as an infinite cosine series in the z-dependence. This suggests a similar dependence for the pressure:

$$\Pi_0(r,z) = p_0 + \sum_{n=1}^{\infty} \Pi_n(r) \cos[x_n(z+\Lambda)], \tag{41}$$

where the $\Pi_n(r)$ satisfy

$$\left[\frac{1}{r}\frac{\partial}{\partial r}\left(r\frac{\partial}{\partial r}\right) - x_n^2\right] \Pi_n(r) = 2B_H \left[\frac{k_0^+ x_n^2 I_1(k_0^+ r) I_1(k_n^- r)}{k_n^- I_0(k_0^+) I_0(k_n^-)} h_n^- + \frac{k_0^- x_n^2 I_1(k_0^- r) I_1(k_n^+ r)}{k_n^+ I_0(k_0^-) I_0(k_n^+)} h_n^+\right], \tag{42}$$

and where we define the magnetic Bond number B_H as

$$B_H \equiv \mu_0 H_0^2 R/2\sigma \tag{43}$$

which is a measure of the relative influence of the magnetic and capillary forces for the static configuration. Notice that B_H may be also expressed in the form $(\omega_A/\omega_c)^2$, with

$\omega_A = (\mu/2\rho)^{\frac{1}{2}}(H_0/R)$ the Alfvén frequency and ω_c the capillary frequency. Here we prefer to stress the role of B_H as the ratio of magnetic to capillary forces and in this respect it is analogous to the classical Bond number, which is the ratio of gravitational to capillary forces.

A particular solution to this ordinary differential equation is obtained by inspection. The general solution which is regular at the symmetry axis is

$$\Pi_n(r) = p_n \frac{I_0(x_n r)}{I_0(x_n)} + B_H x_n^2 \left[\frac{I_0(k_0^+ r) I_0(k_n^- r)}{k_n^{-2} I_0(k_0^+) I_0(k_n^-)} h_n^- + \frac{I_0(k_0^- r) I_0(k_n^+ r)}{k_n^{+2} I_0(k_0^-) I_0(k_n^+)} h_n^+\right] \tag{44}$$

for $n \neq 0$, where the p_n is a new infinite set of integration constants to be determined from the remaining boundary conditions.

Finally, the velocity field is obtained from linearization of (9). Taking the time average of the magnetic force, in non-dimensional form we have for the radial component:

$$\mathrm{i} s v_{0r} \mathrm{e}^{\mathrm{i}st} = -\frac{\partial \Pi_0}{\partial r} \mathrm{e}^{\mathrm{i}st} + 2B_H \left\langle H_S(r,t) \frac{\partial h_{0r}}{\partial z} \right\rangle, \tag{45}$$

where all the time dependences are consistent.

3.3. *Use of the boundary conditions*

The free surface shape $f_0(z)$ is governed by (18), which represents the balance in the normal stress at the interface. This equation is, as usual, made non-dimensional, linearized and finally time averaged to give

$$\left[\frac{\mathrm{d}^2 f_0(z)}{\mathrm{d}z^2} + f_0(z)\right] \mathrm{e}^{\mathrm{i}st} = 2B_H \left\langle \cos\omega t \frac{\partial \phi_0}{\partial z}(1,z) \right\rangle - \Pi_0(1,z)\,\mathrm{e}^{\mathrm{i}st}. \tag{46}$$

We have a second-order ordinary differential equation for $f_0(z)$ whose inhomogeneity appears as a Fourier cosine series. This is a situation already found for the liquid bridge configuration in other contexts, e.g. Sanz (1985) and González *et al.* (1989). In these works the procedure has been to seek a particular solution as another cosine series and to add the solution of the homogeneous equation, which is later expanded on the same cosine complete basis in the interval $[-\Lambda, \Lambda]$. In this way, we are able to express all the remaining boundary conditions over $f_0(z)$ as separate algebraic equations for the Fourier coefficients.

We start this procedure by seeking a particular solution of (46) in the form $\sum_{n=0}^{\infty} a_n \cos[x_n(z+\Lambda)]$. We obtain the following relation for $n \neq 0$:

$$(1-x_n^2)\,a_n = B_H x_n(\phi_n^+ + \phi_n^-) - p_n - B_H x_n^2 \left(\frac{h_n^-}{(k_n^-)^2} + \frac{h_n^+}{(k_n^+)^2}\right) \tag{47}$$

and $a_0 = -p_0$. The solution to the homogeneous equation associated with (46) is

$$f_h(z) = \alpha \sin z + \beta \cos z = \sum_{n=0}^{\infty} r_n \cos[x_n(z+\Lambda)], \tag{48}$$

where $r_0 = \beta \sin(\Lambda)/\Lambda$ and for $n \neq 0$

$$r_n = \begin{cases} \dfrac{2\alpha \cos \Lambda}{\Lambda(1-x_n^2)} & \text{for } n \text{ odd} \\[2ex] \dfrac{2\beta \sin \Lambda}{\Lambda(1-x_n^2)} & \text{for } n \text{ even.} \end{cases} \tag{49}$$

The general solution is then

$$f_0(z) = \sum_{n=0}^{\infty} (a_n + r_n) \cos[x_n(z+\Lambda)]. \tag{50}$$

The volume preservation condition is linearized to give

$$\int_{-\Lambda}^{\Lambda} \mathrm{d}z f_0(z) = 0. \tag{51}$$

Introducing (50) in (51) yields $a_0 + r_0 = 0$, i.e. the summation in (50) actually starts with $n = 1$. Notice that the volume condition gives the value of p_0 once the integration constant β is determined.

From (32) and (33) we obtain new relations among a_n, r_n, $h_n^{\pm}$ and $\phi_n^{\pm}$:

$$\frac{x_n I_1(k_n^{\pm})}{k_n^{\pm} I_0(k_n^{\pm})} h_n^{\pm} = -\frac{x_n K_1(x_n)}{K_0(x_n)} \phi_n^{\pm}, \tag{52}$$

$$x_n \phi_n^{\pm} - h_n^{\pm} = (a_n + r_n) \frac{k_0^{\pm} I_1(k_0^{\pm})}{2 I_0(k_0^{\pm})}. \tag{53}$$

Finally, we linearize the kinematic condition, (14), to give

$$\mathrm{i} s f_0(z) = v_{0,r}(1, z) \tag{54}$$

and substitute the radial velocity from (45). After some algebra the result is

$$s^2(a_n + r_n) = \frac{x_n I_1(x_n)}{I_0(x_n)} + B_H x_n^2 \left[\frac{k_0^+ I_1(k_0^+)}{k_n^- I_0(k_0^+)} h_n^- + \frac{k_0^- I_1(k_0^-)}{k_n^+ I_0(k_0^-)} h_n^+ \right]. \tag{55}$$

Equations (52)–(55) allow us to write all the unknown coefficients in terms of those of the surface shape $a_n + r_n$. We introduce the notation

$$h_n^{\pm} = C_{hn}^{\pm}(a_n + r_n), \quad \phi_n^{\pm} = C_{\phi n}^{\pm}(a_n + r_n), \quad p_n = \frac{I_0(x_n)}{x_n I_1(x_n)} [s^2 + B_H C_{pn}](a_n + r_n), \tag{56}$$

where

$$C_{hn}^{\pm} \equiv -\frac{k_0^{\pm} I_1(k_0^{\pm})}{2 I_0(k_0^{\pm})} \left[1 + \frac{x_n I_1(k_n^{\pm}) K_0(x_n)}{k_n^{\pm} I_0(k_n^{\pm}) K_1(x_n)} \right]^{-1}, \tag{57}$$

$$C_{\phi n}^{\pm} \equiv -C_{hn}^{\pm} \frac{I_1(k_n^{\pm}) K_0(x_n)}{k_n^{\pm} I_0(k_n^{\pm}) K_1(x_n)}, \tag{58}$$

$$C_{pn} \equiv x_n^2 \left| \frac{k_0^+ I_1(k_0^+)}{I_0(k_0^+)} \right|^2 \mathrm{Re} \left\{ k_n^{\pm -2} \left[1 + \frac{x_n I_1(k_n^{\pm}) K_0(x_n)}{k_n^{\pm} I_0(k_n^{\pm}) K_1(x_n)} \right]^{-1} \right\}. \tag{59}$$

Substitution in (47) leads to

$$a_n + r_n = (1 - x_n^2) r_n \left[1 - x_n^2 + \frac{I_0(x_n)}{x_n I_1(x_n)} s^2 + B_H \Gamma_n \right]^{-1}, \tag{60}$$

where

$$\Gamma_n \equiv \frac{I_0(x_n)}{x_n I_1(x_n)} C_{pn} + 2 \,\mathrm{Re}\,(x_n^2 C_{hn}^{\pm} k_n^{\pm -2} - x_n C_{\phi n}^{\pm}). \tag{61}$$

The anchoring condition is written as $f_0(\pm\Lambda) = 0$ or, according to (50),

$$\sum_n (a_n + r_n)(\pm 1)^n = 0.$$

These are two conditions that we add and subtract together to give, using (49):

$$2\alpha \frac{\cos\Lambda}{\Lambda} \sum_{\substack{n=1 \\ \text{odd}}}^{\infty} \left[1 - x_n^2 + \frac{I_0(x_n)}{x_n I_1(x_n)} s^2 + B_H \Gamma_n\right]^{-1} = 0, \tag{62}$$

$$2\beta \frac{\sin\Lambda}{\Lambda} \sum_{\substack{n=2 \\ \text{even}}}^{\infty} \left[1 - x_n^2 + \frac{I_0(x_n)}{x_n I_1(x_n)} s^2 + B_H \Gamma_n\right]^{-1} = 0. \tag{63}$$

If α and β are both zero all the perturbed quantities also become zero and the trivial solution is recovered. Therefore, the expression in brackets must be zero to describe oscillations. Both equations define the natural oscillation frequencies for the cylindrical liquid bridge as a function of the remaining parameters, $s(\Lambda, B_H, d)$. If the applied magnetic field is zero these frequencies become those given in Sanz (1985) for liquid bridges in the absence of an outer bath.

The limit of infinite frequency

Before discussing the above results we shall solve independently the limiting case of infinite frequency of the imposed magnetic field. In this limit we have no penetration of the field into the liquid zone and an azimuthal electric surface current is responsible for the jump in the tangential component of $\boldsymbol{H}$. The time dependence of the applied field may be omitted in the formulation of the problem.

The perturbed magnetic problem reduces to finding the harmonic potential $\phi_0(r,z)\,\mathrm{e}^{\mathrm{i}st}$ outside the conducting liquid whose solution is described by one of ϕ^+ and ϕ^- in (37). We will drop the superindexes in the present analysis. The boundary conditions at $r = f(z,t)$ are now

$$\boldsymbol{n}\cdot\nabla\phi = 0, \quad \boldsymbol{n}\times\nabla\phi = \boldsymbol{K}, \tag{64}$$

where $\boldsymbol{K}$ is the surface current at the interface. The last condition merely gives the value of this new magnitude and is not relevant in our analysis. The linearization of the former gives, in non-dimensional form,

$$\frac{\partial\phi_0}{\partial z}(1,z) = \frac{\mathrm{d}f}{\mathrm{d}z}(z). \tag{65}$$

For the fluid mechanical problem inside the conducting liquid the magnetic forces in the volume disappear in this limit and they are now exerted upon the free surface. We thus have $p^i = p^i_S + \Pi_0(r,z)\,\mathrm{e}^{\mathrm{i}st}$ with

$$\nabla^2 \Pi_0 = 0, \tag{66}$$

whose regular solution is

$$\Pi_0 = p_0 + \sum_{n=1}^{\infty} p_n \frac{I_0(x_n r)}{I_0(x_n)} \cos[x_n(z+\Lambda)]. \tag{67}$$

The normal stress balance at the interface is modified by the existence of a non-zero jump in the Maxwell stress tensor. In non-dimensional form we have

$$p^i - p^o - \tfrac{1}{2}B_H|\boldsymbol{n}\times\boldsymbol{H}^o|^2 = \nabla\cdot\boldsymbol{n}. \tag{68}$$

Linearization of this equation gives

$$\frac{d^2 f_0}{dz^2}(z)+f_0(z) = B_H \frac{\partial \phi_0}{\partial z}(1,z)-\Pi_0(1,z). \tag{69}$$

Finally, the linearized kinematic condition (54) remains valid, where now the radial velocity satisfies $isv_{0,r} = -\partial p_0/\partial r$.

The subsequent analysis is quite similar to the previous one. The final result may be still expressed by (62) and (63) with a new definition of Γ_n:

$$\Gamma_n \equiv -2\frac{x_n K_0(x_n)}{K_1(x_n)}. \tag{70}$$

The equations that governs the system in the limit of infinite frequency are not easily found from those corresponding to the general case by considering the relative penetration depth going to zero. However, if we perform this limit in the final expression taking into account the asymptotic behaviour of the Bessel functions for large arguments in (61) we observe full agreement between both definitions of Γ_n.

It is important to observe that this limit is an exact result beyond the validity range of the inviscid model. In fact it is possible to obtain the stability criterion (independently of the dynamical behaviour of the bridge) from a purely static analysis, as is done for dielectric liquid bridges subjected to axial electric fields in González *et al.* (1989). As the velocity does not enter into the static formulation the result is valid for liquids of arbitrary viscosity.

4. Dispersion relation for the jet

The differences in mathematical treatment between the bridge and the jet are the boundary conditions at $z = \pm\frac{1}{2}\Lambda$ for all magnitudes. The volume equations and conditions at the free surface remain valid. The set of eigenfrequencies is now continuous and we must deal with a dispersion relation relating frequencies and wavenumbers of the disturbances rather than a countably infinite set of natural frequencies. For a linear problem the superposition principle holds and a general perturbation of the interface may be decomposed into independent modes of the form

$$f(z,t) = 1+\mathrm{Re}\,[\epsilon_k\, e^{i(st+xz)}], \tag{71}$$

with $x \equiv kR$ and k the disturbance wavenumber. This assumption is characteristic of a temporal instability approach to the jet dynamics.

The disturbed magnetic and pressure fields are given by

$$\phi_{\pm}(r,z) = \phi_k^{(\pm)} \frac{K_0(xr)}{K_0(x)} e^{i(st+xz)}, \tag{72}$$

$$h_{\pm,z}(r,z) = h_k^{(\pm)} \frac{I_0(\gamma^{\pm} r)}{I_0(\gamma^{\pm})} e^{i(st+xz)}, \tag{73}$$

$$h_{\pm,r}(r,z) = \frac{x h_k^{(\pm)}}{\gamma^{\pm}} \frac{I_1(\gamma^{\pm} r)}{I_0(\gamma^{\pm})} e^{i(st+xz)}, \tag{74}$$

$$\Pi(r) = p_k \frac{I_0(xr)}{I_0(x)} + B_H x^2 \left[\frac{I_0(k_0^+ r)\, I_0(\gamma^- r)}{(\gamma^-)^2 I_0(k_0^+)\, I_0(\gamma^-)} h_k^- + \frac{I_0(k_0^- r)\, I_0(\gamma^+ r)}{(\gamma^+)^2 I_0(k_0^-)\, I_0(\gamma^+)} h_k^+\right], \tag{75}$$

where $\gamma^{\pm} \equiv (x^2 + \mathrm{i}R^2/\delta_{\pm}^2)^{\frac{1}{2}} \approx (x^2 \pm \mathrm{i}R^2/\delta^2)^{\frac{1}{2}}$. Substituting these expressions into the boundary conditions at the free surface (45), (31), (32) and (54) after elimination of v_r from (44), we obtain the dispersion relation

$$1 - x^2 + \frac{I_0(x)}{xI_1(x)} s^2 + B_H \Gamma_k = 0, \tag{76}$$

with Γ_k given by

$$\Gamma_k \equiv \frac{I_0(x)}{xI_1(x)} C_{pk} + 2\,\mathrm{Re}\,(x^2 C_{hk}^{\pm} \gamma^{\pm -2} - x C_{\phi k}^{\pm}) \tag{77}$$

which is obviously connected with (59), and where $C_{\phi k}^{\pm}$, $C_{hk}^{\pm}$ and C_{pk} are defined from (55)–(57) by making the substitutions x and $\gamma^{\pm}$ instead of x_n and $k_n^{\pm}$ respectively.

Let us consider the limit of infinite radius in (76). The intervening Bessel functions have arguments proportional to R and may be substituted by unity in the limit because they always appear as quotients of two functions of the same kind and argument. In this limit we have (with explicit dependence on R)

$$C_{hk}^{\pm} \to -\frac{R(\pm \mathrm{i})^{\frac{1}{2}}}{2\delta}\left(1 + \frac{a}{(a^2 \pm \mathrm{i})^{\frac{1}{2}}}\right)^{-1}, \tag{78}$$

$$C_{\phi k}^{\pm} \to \frac{(\pm \mathrm{i})^{\frac{1}{2}}}{2(a^2 \pm \mathrm{i})^{\frac{1}{2}}}\left(1 + \frac{a}{(a^2 \pm \mathrm{i})^{\frac{1}{2}}}\right)^{-1}, \tag{79}$$

$$C_{pk} \to (kR)^2\,\mathrm{Re}\,[(a^2 \pm \mathrm{i} + a(a^2 \pm \mathrm{i})^{\frac{1}{2}})^{-1}] \tag{80}$$

with the new parameter $a \equiv k\delta$. Notice that this dimensionless wavenumber is $1/\sqrt{2}$ times that defined by Garnier & Moreau in their work. In dimensional form we arrive at the dispersion relation for a planar interface:

$$\rho s^2 = \sigma k^3 + \tfrac{1}{2}\mu_0 H_0^2 k^2 F(a), \tag{81}$$

where

$$F(a) \equiv -\mathrm{Re}\left[\frac{1}{a^2 \pm \mathrm{i} + a(a^2 \pm \mathrm{i})^{\frac{1}{2}}} - \frac{(\pm \mathrm{i})^{\frac{1}{2}}}{(a^2 \pm \mathrm{i})^{\frac{1}{2}}}\right], \tag{82}$$

which is the same function for the dependence on the penetration length as in Garnier & Moreau's work.

5. Results

We start this section with the analysis of the dispersion relation for the jet. In figure 2 the square of the frequency is plotted as a function of the non-dimensional wavenumber $x = kR$ for fixed relative penetration length $d = 0.1$ and different values of the magnetic Bond number, B_H. Negative squared frequencies imply exponentially growing behaviour, which is characteristic of long-wavelength disturbances in jets. The curve with $B_H = 0$ was obtained by Rayleigh (1945) for axisymmetric capillary jets. We observe that the region of unstable wavenumbers decreases as the magnetic field increases. In figure 3 we illustrate the stabilizing effect of decreasing the penetration length for a given magnetic Bond number ($B_H = 10$). For $d = 5$, i.e. a situation with a weakly non-uniform field inside the conducting liquid, the unstable region virtually covers the entire region $k < 1$, as in the absence of magnetic forces. The curve corresponding to $d = 0.01$ is representative of the case of no penetration (infinite applied frequency).

Consequently, the main effect of the magnetic forces is to stabilize the jet by

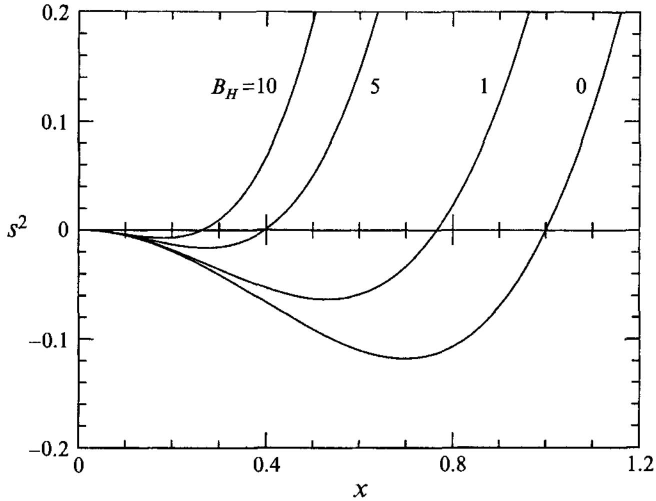

FIGURE 2. Dispersion relation for the jet. s^2 and x are the dimensionless squared oscillation frequency and the wavenumber respectively. The relative penetration length is $d = 0.1$ for all the curves, which have been obtained for different magnetic Bond number.

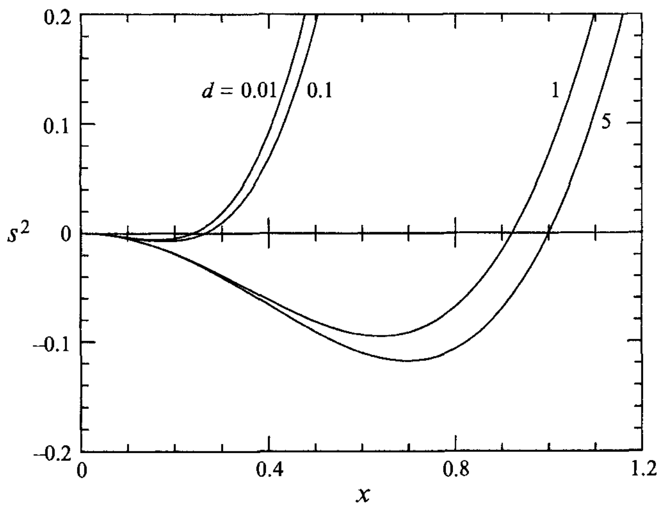

FIGURE 3. Dispersion relation for $B_H = 10$ and different d.

decreasing the most unstable wavenumber (minima of the curves) and the growth factor $|s^2|^{\frac{1}{2}}$ associated with it. The mechanism is most effective in the limit of zero field penetration.

Figure 4 shows the radial dependence of v_r, the radial component of the velocity field, for $x = 1$, $B_H = 10$ and three different values of the relative penetration length d. As this latter parameter decreases, the velocity profile suffers stronger variations near the free surface. This phenomenon enhances the role of the viscosity in the dynamics of the liquid column for very high field frequencies. From the dependences on the variables r and z, it is clear that the velocity field is organized in toroidal rolls of length $2\pi R/x$. The change in sign of the function $v_r(r)$ observed for small d in figure 4 implies the appearance of a secondary roll near the free surface circulating in the opposite direction, its width decreasing as this parameter decreases.

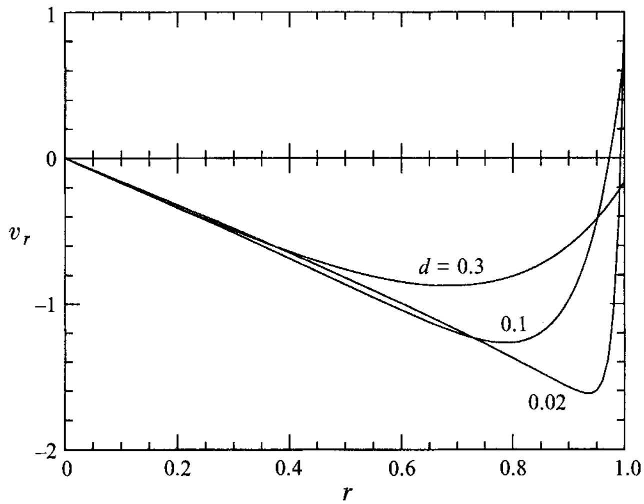

FIGURE 4. Radial dependence of the radial component of the velocity field for the jet. The curves are calculated for $B_H = 10$, non-dimensional wavelength $x = 1$ and different values of d. The formation of a boundary layer near the free surface is clearly shown.

In the case of liquid bridges, the natural frequencies are obtained from the implicit relations given by (62) and (63). Owing to the non-dissipative nature of the model we may demonstrate that s^2 must be real, as in the case of zero applied field (Sanz 1985). For $s^2 > 0$ there is oscillatory behaviour and for $s^2 < 0$ the perturbations grow exponentially, i.e. there is instability to infinitesimal disturbances.

The functions dependent on s, Λ, B_H and d that give these implicit equations are infinite series that must be conveniently approximated. The method followed was to obtain asymptotic expressions for the general term for large n that may be approximated as a sum of a few terms (four in our computations) whose dependence on n is proportional to $1/n^l$, where l is a positive integer greater than or equal to two. The larger number of asymptotic terms taken into account, the better is the convergence of the method. Only a number of terms of the original infinite series is exactly computed, say N (dependent on the particular values of Λ and d). The remaining terms forming the 'queue' are related to the Riemann functions $\zeta(l)$ and they are calculated from tables (Abramowitz & Stegun 1972).

The implicit equations are solved using the Newton–Raphson method. For this purpose it is important to realize that for fixed values of Λ, B_H and d the infinite series has a structure of alternating zeros and singular points like the function $\tan s$. As the singular points are those given by each term in the infinite series, we can easily determine bounded regions where only one zero exists. Each zero s_m, where the subindex is an ordering parameter, corresponds to a solution of (62) or (63) and represent a natural oscillation frequency (or growth factor) of the interface. The shape and associated magnetic, pressure and velocity fields are obtained by putting $s = s_m$ in the corresponding expressions. The resulting shapes are even or odd functions of z, so we have respectively two infinite families of antisymmetric and symmetric normal modes with respect to the plane $z = 0$. There is linear stability for those values of the parameters that make positive all the squared natural frequencies s_m^2. All these properties are well known from the dynamics of cylindrical inviscid liquid bridges for zero applied field (Sanz 1985). In this latter case the slenderness can be considered an ordering parameter because, if we increase it, all the numbers s_m^2 decrease until they

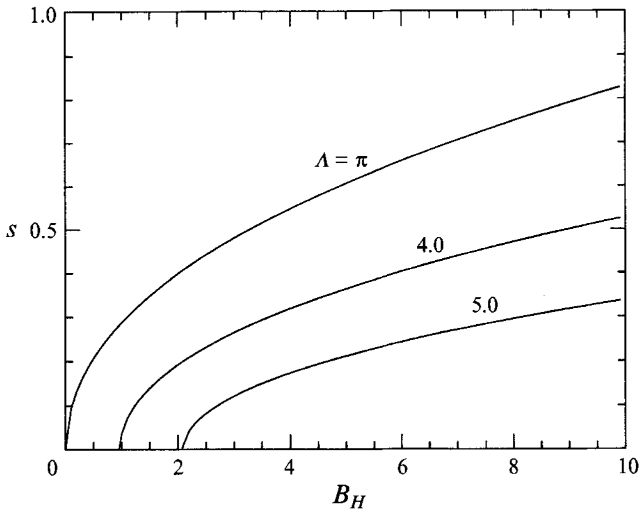

FIGURE 5. Natural frequency s of the axisymmetric mode, as a function of the magnetic Bond number for different values of the slenderness. Here only the case of zero relative penetration length ($d = 0$) is considered.

become negative consecutively. The first value of the slenderness for which we have at least one negative value of the squared natural frequencies is $\Lambda = \pi$, i.e. the classical result given by Rayleigh for the capillary instability of a jet, also valid for a cylindrical liquid bridge. This mode is characterized by an amphoric profile, i.e. a sole node. As a general rule, the destabilization order m of the modes as Λ increases coincides with the number of nodes of $f_0(z)$.

In the case of a non-zero applied magnetic field these features remain valid. However, we observe a general increase in all the natural frequencies as the field intensity increases. This conclusion is apparent from figure 5, where we represent the frequency corresponding to the first destabilized mode as a function of the magnetic Bond number for infinite imposed field frequency or perfectly conducting liquids ($d = 0$) and selected values of the slenderness Λ. Other less dangerous modes exhibit similar behaviour as the field intensity increases and we do not present them. Instability occurs at $s = 0$ along each curve.

Concerning the role of the relative penetration depth d, we may state as a general tendency that s_m^2 decreases as the field penetration increases. In figure 6 we illustrate this fact by representing again the most dangerous mode frequency s_1 for $B_H = 10$ and some values of Λ. The highest frequency is always found for $d = 0$ and it decreases with d increasing. The first natural frequency for $\Lambda = \pi$ goes to zero asymptotically as d goes to infinity, showing that this case is stable even when the field inside the conductor becomes uniform and steady. All these features are in accordance with the results discussed for the jet and with the conclusions given by Garnier & Moreau (1983). For their planar geometry the field increases the frequency of disturbances propagating in its direction. In our configuration, we may consider the surface perturbations as a combination of the infinite-column k-modes, satisfying both anchoring conditions. If so, each particular mode would have its frequency increased, according to figures 2 and 3. Following this analogy, azimuthal modes in cylindrical geometry correspond to disturbances that are normal to the imposed magnetic field and they should not be affected by the field. These non-axisymmetric modes are stable in the absence of magnetic fields and their study does not seem to be relevant.

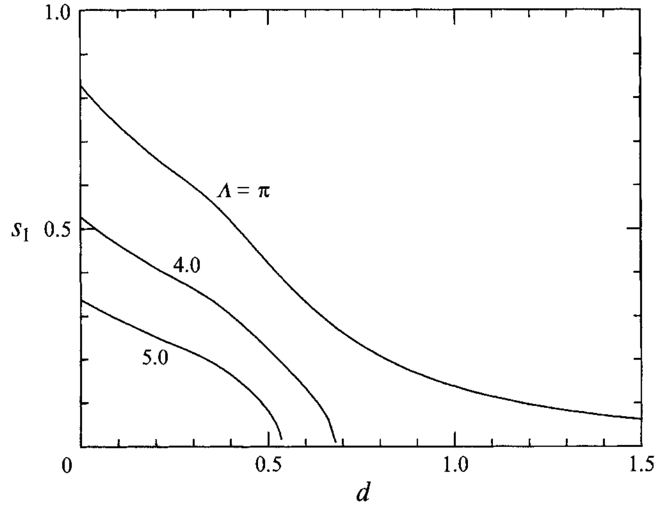

FIGURE 6. Natural frequency s_1 of the axisymmetric mode, as a function of the relative penetration length d, for fixed magnetic Bond number $B_H = 10$ and several values of the slenderness.

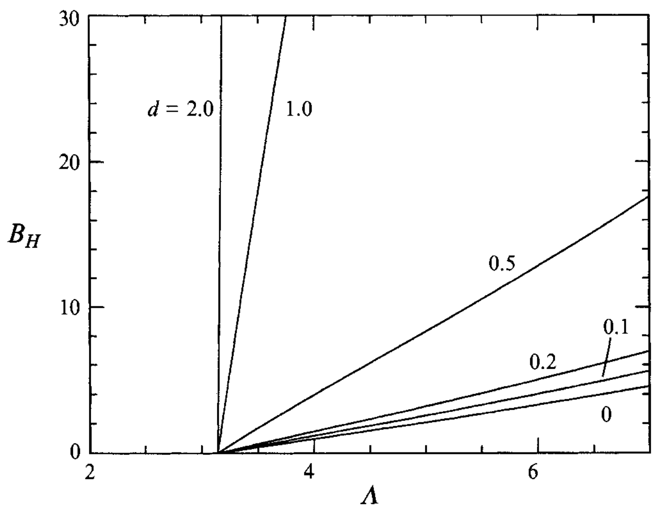

FIGURE 7. Stability curves in the $\Lambda - B_H$ plane for different values of the relative penetration length d. The case $d = 2$ already approximates that of perfect insulators, whilst the case $d = 0$ corresponds either to the case of infinite frequency (non-zero finite electrical conductivity) or to perfectly conducting fluids (non-zero finite frequency).

The consequence of the increase in the natural frequencies with the applied magnetic field is to generally increase the critical slenderness for which there is neutral stability, i.e. $s_1^2 = 0$. In other words, the field has always a stabilizing effect on the liquid bridge. This effect decreases with an increase of the field penetration depth. In figure 7 the neutral stability curves in the (B_H, Λ)-plane for different values of d are presented. Bridges with values of the parameters lying above the curves are stable and, conversely, those under these curves are unstable. The crucial role played by the relative penetration length is apparent from a comparison between the cases $d = 0$ and 2. Another perspective of the parameter space is given in figure 8, where we represent the

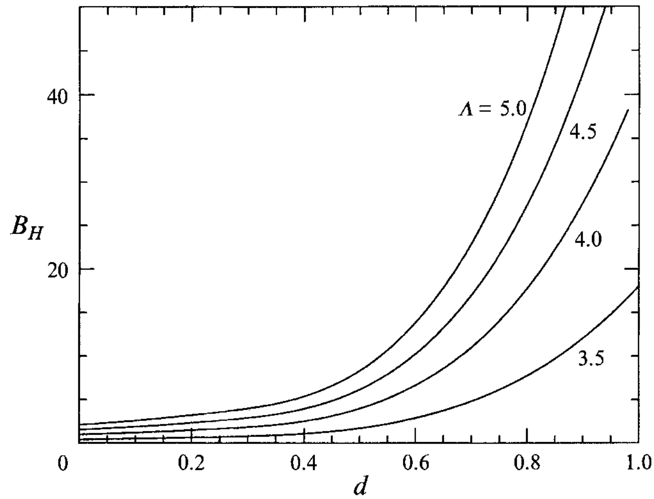

FIGURE 8. Stability limits in the $d-B_H$ plane for different values of the slenderness. Stable configurations correspond to points in the upper regions. For fixed slenderness the necessary value of B_H to stabilize the liquid bridge decreases as d decreases.

stability boundaries in the plane d, B_H for several values of the slenderness. It is apparent that, for $d = 0$ and over a not very narrow range of penetration lengths, the magnetic field is very effective in stabilizing long liquid bridges.

To give an idea of the stabilizing effect we may again consider a cylindrical liquid bridge of radius $R = 2$ cm made of molten silicon. Typical frequencies for the alternating magnetic fields used in the floating-zone technique to grow single crystals are 4 MHz (Keller & Mühlbauer 1981). If we consider a much lower frequency, say 10^5 Hz we have, as given in the introduction, a penetration depth $\delta = 10^{-3}$ m and, relative to the radius of the cylinder, $d = 0.05$. For this value the critical Bond number that makes a liquid bridge of slenderness $\Lambda = 6$ stable is $B_H = 3.62$. The corresponding peak magnetic field intensity is $B_0 = \mu_0 H_0 = 0.019$ T, certainly a moderate intensity. Values two orders of magnitude larger than B_0 are normally used in laboratories. Therefore it could be interesting to test the ability of these magnetic fields to stabilize the melted zone in the floating zone technique.

6. Conclusions

A linear inviscid model to investigate the dynamics and stability of liquid metal or molten semiconductor columns in the presence of an axial alternating magnetic field has been presented. The results could be of interest in understanding the stabilizing effect of these fields in the context of the floating-zone technique, where a radio-frequency magnetic field generated by a circular coil is present. Observations made in connection with this technique show that the liquid zone is slenderer than expected (Keller & Mühlbauer 1981). It has been shown that even for moderate magnetic fields stabilization beyond the Rayleigh limit $\Lambda = \pi$ can be easily achieved if the relative penetration length is small. The penetration of the field inside the conductor decreases with an increase in the frequency or the electrical conductivity, and this feature is responsible for the increase in stability.

The validity of the inviscid model is determined by estimation of a Reynolds number with R/t_c as the velocity scale and the penetration length of the magnetic field inside the conductor as the lengthscale. High-frequency fields give magnetic forces confined to a narrow layer near the free surface. Rapid variations of the radial velocity in this skin-depth layer cause the viscous forces to be not negligible. In spite of this limitation, the case of infinite frequency, giving superficial electric currents, is valid for arbitrary viscosity.

The stabilization mechanism in the case of magnetic fields originates from the opposition of the liquid metal (or molten semiconductor) to the variation of the magnetic flux across the shape caused by its deformation. For alternating magnetic fields the flux variation is directly proportional to the frequency. A different situation arises in the case of the application of static magnetic fields. In the latter situation the convective term in (13) is the dominant one. Therefore our results cannot be extended to very low frequencies. In the limit of zero frequency Chandrasekhar has shown that liquid metals and molten semi-conductors behave as almost perfect insulators, contrary to a naïve expectation. This should not imply that steady magnetic fields are useless in the float-zone technique as it is well known that d.c. fields tend to suppress convection in the melted zone (Baumgartl 1992). Thus an induction coil with a mean continuous component may help the process in two ways: stabilizing the free interface (a.c. component) and inhibiting the Marangoni induced convection in the melt (continuous component).

We acknowledge the commentaries of the referees as we consider that they have significantly improved this work. This research has been supported by the Dirección General de Ciencia y Tecnología (DGCYT), a Spanish Government agency, under contract PB90-0905.

REFERENCES

ABRAMOWITZ, M. & STEGUN, I. 1972 *Handbook of Mathematical Functions*. Dover.

BAUMGARTL, J. 1992 Numerische und experimentelle untersuchungen zur wirkung magnetischer felder in krystallzuchtungsanordnungen. Thesis, Technical Faculty, Erlangen University, Germany.

CHANDRASEKHAR, S. 1961 *Hydrodynamic and Hydromagnetic Stability*. Oxford University Press.

GARNIER, M. & MOREAU, R. 1983 Effect of finite conductivity on the inviscid stability of an interface submitted to a high-frequency magnetic field. *J. Fluid Mech.* **127**, 365–377.

GONZÁLEZ, H., MCCLUSKEY, F. M. J., CASTELLANOS, A. & BARRERO, A. 1989 Stabilization of dielectric liquid bridges by electric fields in the absence of gravity. *J. Fluid Mech.* **206**, 545–561.

HURLE, D. T. J., MÜLLER, G. & NITSCHE, R. 1987 Crystal growth from the melt. In *Fluid Sciences and Materials Science in Space* (ed. H. U. Walter). Springer.

KELLER, W. & MÜHLBAUER, A. 1981 *Floating-Zone Silicon*. Marcel Dekker.

MARTÍNEZ, I. & CRÖLL, A. 1992 Liquid bridges and floating zones. *ESA-SP* 333, 135–142.

NICOLÁS, J. A. 1992 Magnetohydrodynamic stability of cylindrical liquid bridges under a uniform axial magnetic field. *Phys. Fluids* A **4**, 2573–2577.

RAYLEIGH, LORD 1945 *The Theory of Sound*, vol. 2. Dover.

RIAHI, D. N. & WALKER, J. S. 1989 Float zone shape and stability with the electromagnetic body force due to a radio-frequency induction coil. *J. Cryst. Growth* **94**, 635–642.

SANZ, A. 1985 The influence of an outer bath in the dynamics of axisymmetric liquid bridges. *J. Fluid Mech.* **156**, 101–140.